

Dynamics of metal clusters in rare gas clusters

M. BAER

*Institut für Theoretische Physik, Universität Erlangen, Staudtstrasse 7,
D-91058 Erlangen, Germany*

G. BOUSQUET, P.M. DINH*

*Laboratoire de Physique Théorique, UMR 5152, Université P. Sabatier 118 Rte de Narbonne,
F-31062 Toulouse cedex, France*

**E-mail: dinh@irsamc.ups-tlse.fr*

F. FEHRER, P.-G. REINHARD**

*Institut für Theoretische Physik, Universität Erlangen, Staudtstrasse 7,
D-91058 Erlangen, Germany ,*

***E-mail: mpt218@theorie2.physik.uni-erlangen.de*

E. SURAUD

*Laboratoire de Physique Théorique, Université P. Sabatier 118 Rte de Narbonne,
F-31062 Toulouse cedex, France*

We investigate the dynamics of Na clusters embedded in Ar matrices. We use a hierarchical approach, accounting microscopically for the cluster's degrees of freedom and more coarsely for the matrix. The dynamical polarizability of the Ar atoms and the strong Pauli-repulsion exerted by the Ar-electrons are taken into account. We discuss the impact of the matrix on the cluster gross properties and on its optical response. We then consider a realistic case of irradiation by a moderately intense laser and discuss the impact of the matrix on the hindrance of the explosion, as well as a possible pump probe scenario for analyzing dynamical responses.

Keywords: Metal cluster, rare gas matrix, laser irradiation, Density Functional Theory

1. Introduction

Structural and dynamical properties of clusters, especially in the case of simple alkali clusters, have focused many experimental as well as theoretical investigations.¹⁻⁵ The case of clusters embedded in a matrix or deposited on a surface requires specific treatments, because the environment influences cluster properties and has thus to be incorporated in the analysis. It should nevertheless be noted that the presence of an environment (surface or matrix) may simplify the experimental handling: it usually implies localization, fixed geometry, well controlled temperature, and higher yields. Deposited and/or embedded clusters thus often represent a preferred alternative

for cluster studies. But the presence of an environment complicates the theoretical modeling. It requires a handling of the cluster-matrix interface and the huge number of atoms in the matrix or substrate may become prohibitive. But because many interesting experiments have been, or can only be, done with clusters in contact with a carrier material such theoretical investigations, although challenging, become unavoidable. Let us mention as examples of experimental motivations the systematics of optical response in large noble-metal clusters^{6,7} and its dependence on the environment.⁸

While static properties of embedded/deposited clusters have already been studied since long,^{2,3} dynamical scenarios still remain little explored⁵ but promise challenging questions. As in free clusters, the optical response represents a key tool of analysis, both of cluster structure, in particular in metal clusters¹ and in most dynamical situations. Let us mention the case of moderate perturbations, as, *e.g.*, in the case of laser irradiation in which resonant coupling between laser and cluster eigenfrequencies represents a basic doorway mechanism for many dynamical scenarios.⁵ The study of the optical response thus constitutes a key "entry point" for the cluster response to electromagnetic probes.

Among the various possible combinations of clusters with substrate/matrix, the case of inert or moderately active environments is especially interesting. It implies only moderate perturbations of cluster properties and one can thus still benefit from the well defined geometry of the system and access predominantly the cluster properties themselves. From the theoretical side, the environment can be included at a lower level of description (hierarchical method), which simplifies the handling. This is the type of situations we shall focus on in the following, namely the case of simple metal clusters (sodium) inside a moderately active environment (rare gas matrix).

The term "hierarchical method", used above, requires some comments. It refers to the fact that the interface may be treated at a simpler level than the cluster's degrees of freedom, because of the moderate interactions between cluster and environment. Such approaches are well known in many complex systems, as for example the shell model in surface chemistry^{9,10} or the coupled quantum-mechanical with molecular-mechanical method (QM/MM) often used in bio-chemistry.¹¹⁻¹³ Hierarchical modeling is nevertheless not free from difficulties, especially at the technical side, because the interface interaction requires a very careful adjustment. And this may become very tough when one is dealing with a huge range of energies (cluster *vs.* matrix), as in the case of an alkaline cluster embedded in a rare gas (RG) matrix, where one has to deal with eV (Na) as well as meV (RG-RG and RG-Na). But once properly tuned the model becomes able to simulate rather easily realistic situations, especially in terms of system's sizes.

The paper is organized as follows. A brief presentation of the hierarchical approach is given in section 2. We then discuss the impact of the matrix on gross properties of a small metal cluster. We then pursue the analysis by considering the impact of the matrix on the optical response of the embedded cluster. We finally

illustrate possible violent irradiation scenarios on a realistic example.

2. Model

The model has been presented in detail in¹⁴ and we just remind here the basic ingredients. The Na cluster is described in the TDLDA-MD approach, an approach which has been validated for linear and non-linear dynamics of free metal clusters.^{5,15} It combines a (time-dependent) density-functional theory at the level of the local-density approximation (TDLDA) for the electrons, to a classical molecular (MD) dynamics for the ions. The electron-ion interaction is described by soft, local pseudo-potentials.¹⁶ Two classical degrees-of-freedom are associated with each Ar atom : its center-of-mass and its electrical dipole moment. The dipoles allow to explicitly treat the dynamical polarizability of the atoms with help of polarization potentials.¹⁷ The atom-atom interactions are described by a standard Lennard-Jones potential, and for the Ar-Na⁺ subsystem we employ effective potentials from the literature.¹⁸ The pseudo-potential for the electron-Ar core repulsion has been modeled in the form proposed by,¹⁹ and we slightly readjust it by a final fine-tuning to the NaAr molecule as benchmark (bond length, binding energy, and optical excitation). A Van der Waals interaction is also added and computed *via* the variance of dipole operators.^{14,19,20}

The starting quantity is the total energy which is constructed from the various pieces as outlined above. From the total energy, the corresponding equations of motion can be derived by standard variation. This leads to the time-dependent Kohn-Sham equations for the cluster electrons. And one obtains Hamiltonian equations of motion for the classical degrees of freedom (namely Na⁺ ions and Ar atom positions and dipoles). The initial condition is obtained from the corresponding stationary equations. The Ar-sodium configuration is produced as follows. One cuts a finite piece from a fcc Ar crystal and optimizes the structure. One then carves a central cavity to place the Na cluster inside. The total configuration is then re-optimized by means of cooled molecular dynamics for the ions and atoms coupled to stationary Kohn-Sham solution for the cluster electrons.

We compute several observables to analyze the statics and dynamics of the system. The ionic and electronic cluster structure is characterized in terms of r.m.s. radii

$$r_{I,e} = \sqrt{\langle (x^2 + y^2 + z^2) \rangle_{I,e}} \quad (1)$$

where $\langle . \rangle_I = \sum_I . / N_I$ and $\langle . \rangle_e = \int d^3r . \rho_e(\mathbf{r}) / N_e$. We also analyze the shape of the system by computing the reduced quadrupole moment β_2 which reads

$$\beta_2 = \frac{4\pi}{5} \frac{\sqrt{\frac{5}{16\pi}} \langle (2z_I^2 - x_I^2 - y_I^2) \rangle_{I,e}}{\langle r^2 \rangle_{I,e}} \quad (2)$$

with obvious notations. The optical response is obtained from the dipole moment $D_{el} = \langle \sum_n z \rangle$ as quantum mechanical expectation value over the Kohn-Sham state.

The dynamics is initiated by an instantaneous dipole boost of the cluster electrons. The dipole signal is followed in the time domain $D_{e1}(t)$ and then Fourier transformed to the frequency domain to obtain the dipole strength as imaginary part of the Fourier transformed dipole moment.²¹⁻²³

The numerical solution proceeds with standard methods as described in detail in.¹⁵ The (time-dependent) Kohn-Sham equations for the cluster electrons are solved using real space grid techniques. The time propagation proceeds using a time-splitting method, and the stationary solution is attained by accelerated gradient iterations. We furthermore employ the cylindrically-averaged pseudo-potential scheme (CAPS) as introduced in,^{24,25} which is justified for the chosen test cases. The Na^+ ions as well as the Ar atoms are nevertheless still treated in full 3D.

3. Gross properties of embedded clusters

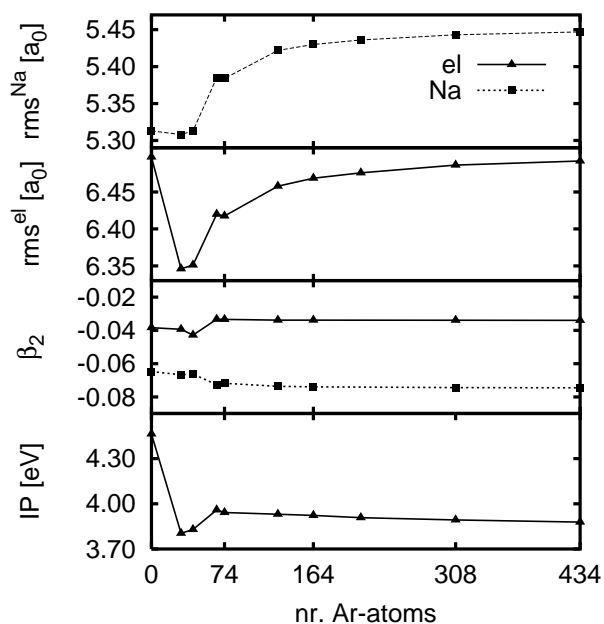


Fig. 1. Trend of basic observables with matrix size: ionic and electronic r.m.s. radius, ionic and electronic quadrupole deformation β_2 , electronic ionization potential (IP). The matrix is optimized anew for each configuration. From.¹⁴

We take as test case a Na_8 cluster embedded into an Ar matrix of various sizes. Fig. 1 summarizes a few basic properties of the embedded cluster as a function of increasing matrix size. For moderate size matrices the electronic radius is first reduced (as compared to the free cluster), because of the strong repulsive Ar-core potentials. But with increasing matrix size both the electronic and the ionic radii

expand in a similar way because of the monopole-dipole interaction between Na^+ and the Ar-atoms. The global deformation (third panel from top in Fig. 1) is nearly independent of matrix size, although one can spot a slight trend for small sizes. The ionization potential (IP) is, as usual, defined as the energy difference between Na_8 and Na_8^+ for ionic and atomic positions frozen. The IP globally exhibits a decrease mostly due to the short range compression. There is indeed a big jump from the free to the clusters inside small matrices and very little changes amongst all embedded systems, in accordance with the short-range nature of the Ar core potentials. Generally speaking one can identify from the figure two regimes, with a threshold at 164 Ar atoms. Below that limit one observes specific size effects, which tend to be smoothed out for larger sizes for which one observes a monotonous trend towards the asymptotic value. This again reflects the balance between the two competing effects, namely the short range repulsion due to compression effects and the long range attraction due to polarization effects.

4. Linear optical response

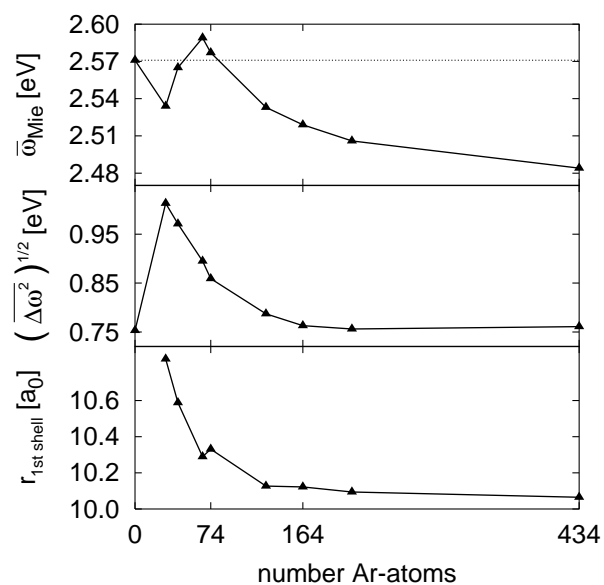


Fig. 2. Average peak position, width and radius of the innermost Ar shell, as a function of matrix size. From.¹⁴

Fig. 2 presents the trend of the average plasmon peak position $\bar{\omega}_{\text{Mie}}$ and width $(\Delta\omega^2)^{1/2}$ with matrix size, as well as the radius of the innermost Ar shell. The value $\bar{\omega}_{\text{Mie}}$ is the averaged dipole transition over the interval [1.9 eV; 3.2 eV]. The width is the variance of the frequency computed in the same averaging interval. Once again,

visible structures are seen only below 164 Ar atoms. While the Na_8 exhibits a clean Mie plasmon peak, spectral structures of the clusters embedded in small matrices are strongly fragmented, corresponding to a larger width (see middle panel). This effect is clearly due to Landau fragmentation, since the surrounding Ar atoms modify the spectral density of one-electron-one-hole states near the resonance. Indeed the latter emerges from a subtle interplay of core repulsion and dipole attraction. For matrices larger than 164 Ar atoms, the variance decreases rapidly and saturates at the same value as that of the free Na_8 , leading to a fairly clean plasmon peak again.

Note however that the changes in the average resonance position are very little or even insignificant, that is, less than 1/10 of an eV. This is the result of an almost complete cancellation of core and polarization potentials.¹⁴ Indeed we have computed the dipole spectrum for $\text{Na}_8\text{Ar}_{164}$ while switching off the polarization potentials from the Ar atoms. Thus the cluster electrons feel only the repulsion of the Ar core potentials. The effect is a strong blue-shift of the resonance by about 0.8 eV. Switching on the polarization potentials produces an equally strong red-shift. At the end, the peak position comes out almost unchanged as compared to the free cluster. It is obvious that the final resonance position, resulting from two large and counteracting effects, is extremely sensitive to details of the model. One should thus be careful not to overinterpret the trends at the meV scale.

Looking back to Fig. 2 with that mechanism in mind, the radius of the innermost Ar shell shrinks strongly up to about 74 atoms (bottom panel). This corresponds to the regime where core repulsion increases. The dipole attraction increases as well and we see practically constant average peak position. For larger systems, whereas the core effect stabilizes, the dipole attraction still increases, although on a lower rate. This explains why a small but steady red-shift is seen for further increasing system sizes. We have estimated the effects for further shells towards the full crystal and we found about 14 meV more red-shift asymptotically. It is a systematic effect, but a very small one. Thus we will ignore it for the now following explorations of violent excitations.

5. Strongly excited Na cluster in an Ar environment

In this section, we present a realistic intense laser excitation of the system $\text{Na}_8\text{@Ar}_{434}$. The laser features are the following: polarization along the symmetry axis of the system (and denoted below as the z axis), frequency of 1.9 eV, intensity of $2 \times 10^{12} \text{ W}\cdot\text{cm}^{-2}$ and FWHM of 50 fs. The system reacts mainly by a strong dipole moment which leads to a direct emission of 3 electrons which escape instantaneously (i.e. within 3-10 fs). One may wonder whether the strong external or effective Coulomb field at Ar sites would also trigger electron emission from Ar. This was checked by TDLDA calculations for an Ar atom and we found a critical field strength of about $0.1 \text{ Ry}/a_0$ for that process. In our calculations, we record the actual field strengths at all Ar sites. They stay safely below this critical value all times. Electron emission thus comes exclusively from the Na cluster ($\text{Na}_8 \rightarrow \text{Na}_8^{3+}$).

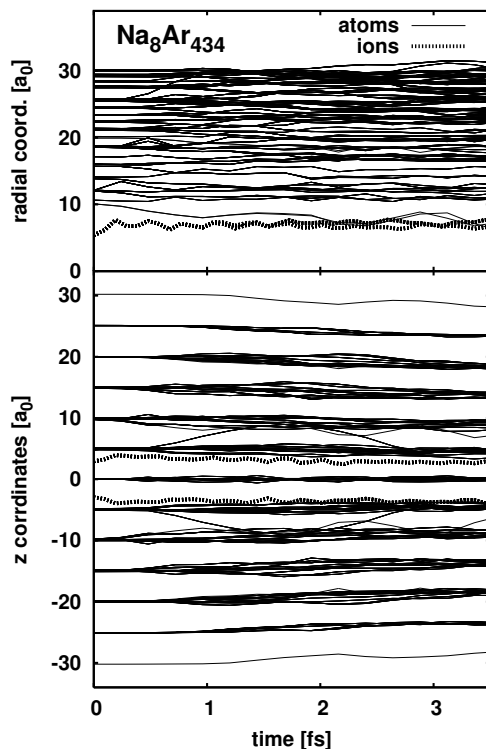


Fig. 3. Time evolution of the the atomic (full lines) and ionic (dotted lines) z -coordinates (lower panel) and radial distances $r = \sqrt{x^2 + y^2 + z^2}$ (upper panel) for $\text{Na}_8\text{Ar}_{434}$ excited with a laser (see text for details).

In Fig. 3, showing the time evolution of the Na ions and Ar atoms coordinates, we observe a rearrangement of the whole system at ionic/atomic time scale, due to the thus produced large Coulomb pressure. We note however different interesting time scales. First the Na ions start, up to about 200 fs, a Coulomb explosion, almost identical to the similar case of a free Na_8 cluster lifted to charge 3^+ . Second when the ions hit the repulsive core of the first shell of Ar, the “explosion” is abruptly stopped. Then the ionic motion turns to damped oscillations around a (r.m.s.) radius of about $7 a_0$. Note that the shape oscillations of the cluster have the typical cycle of about 250 fs, well known for free Na clusters²⁶ and re-established for embedded ones.²⁷

Two stages in the matrix are also seen, although on longer time scales. We first observe a “diffusion” of the perturbation (due to rearrangement of Na ions) into the various Ar shells. This is especially visible along the z axis which allows to read off the propagation speed of this perturbation as $20\text{-}30 a_0/\text{ps}$. We have estimated the sound velocity in the corresponding large pure Ar cluster (Ar_{447}) by computing its vibrational spectrum. The radial compression mode corresponds to the sound mode

in bulk material. We found a frequency of $\omega_{\text{vib}} = 1.8$ meV. The momentum of the radial wave is $q = \pi/R$ where $R = 30$ a_0 is the cluster radius. The sound velocity is then estimated as $v_{\text{sound}} = \omega_{\text{vib}}/q \approx 30$ a_0/ps which is very close to the propagation speed as observed in the figure. One may thus interpretate the perturbation as a sound wave sent by the initial bounce of the Na ions.

Then the perturbation generates oscillations combined with some diffusion which, after about 1.5 ps, has spread over all shells. Even the outermost shell is perturbed and the matrix seems to get an oblate deformation, as the Na_8 does. However whereas the Na cluster exhibits a global relaxed trend to oblate shapes, the relaxation of the Ar atoms seems much longer than that of the Na ions and far beyond the time scale computed here. These long time scales for full relaxation and evaporation of Ar atoms are well known from experiments of dimer molecules embedded in Ar clusters, see *e.g.*²⁸

Let us now briefly comment on the finite net charge of our system. It emerges because the electrons propagate almost unhindered through the surrounding Ar cluster and eventually escape to infinity. We may wonder whether, in a macroscopically large matrix, the electrons would be stuck somewhere in the range of their mean free path, drift very slowly back towards the now attractive cluster well, and eventually recombine there. This has been checked by using reflecting boundary conditions rather than absorbing ones. Up to 4 ps, no recombination has been observed. Furthermore the ionic/atomic rearrangements following the irradiation turn out to be qualitatively very similar whatever the boundary conditions. Thus the present scenario should provide a pertinent picture for a few ps, the time window studied here.

Finally one may wonder how to analyze the key pattern of the embedded cluster dynamics experimentally. The energy transfer to the Ar part could be measured from the Ar evaporation spectra as long as one deals with metal clusters embedded in finite Ar drops. But the most interesting effect is the hindered explosion of the imprisoned Na cluster and its subsequent shape oscillations in the Ar cavity. Here we can exploit the pronounced features of the Mie plasmon resonance of the embedded metal cluster. Indeed, it couples strongly to light, the coupling is highly frequency selective, and the plasmon frequencies are uniquely related to the cluster shape. This suggests to track the shape oscillations by pump and probe analysis. In free clusters, a proper setup allows to map in a unique fashion the evolution of radial shape²⁹ and of quadrupole deformations,³⁰ through the time evolution of the Mie plasmon resonance. We have computed that for the case considered here. We take the instantaneous configuration at a given time and compute the optical response in all three spatial directions for the actual charge state of the system. The strong oblate deformation leads to a splitting of the resonance peak where the shorter extension along z is associated to a blue-shift of the mode and the larger extension in orthogonal direction to a red-shift. Our findings are in qualitative agreement with experimental results obtained for Ag in glass,³¹ using a similar pump probe scenario. Our model thus provides a microscopic interpretation, the first one, to the

best of our knowledge, of these experimental investigations.

6. Conclusion

We have presented a robust model for the description of simple Na clusters embedded in an Ar matrix. The dynamics of the Na cluster is treated in the TDLDA-MD *ab initio* framework, allowing any dynamical regime (linear and non-linear) at the side of the Na cluster. The matrix is treated at the simplest level of modeling still accommodating polarization and full MD motion at the side of Ar atoms. Both sodium and argon are properly coupled following previous detailed quantum chemistry calculations. On the basis of that model, we have investigated the structure and dynamics (low and high energy) of the embedded Na cluster.

We have considered in this paper different systems, namely $\text{Na}_8@Ar_n$ with n varying from 0 to 434. The optical response provides an experimental access to the cluster's structure. When the cluster is embedded, the peak position results from a subtle cancellation between two large effects : matrix compression of the ionic configuration, which tends to blue-shift the response, and electronic polarization effects which tend to red-shift the response. All in all the net result, in large matrices, comes very close to the free response. This, by the way, also holds true in the non-linear domain of the plasmon response where the same cancellation effect is found to persist. These results are actually quite compatible with related experiments on Ag in rare gas matrices where it was found that the plasmon peak is very little modified as a function of matrix size. The effect of matrix size was also explored in more detail and some results presented. Again the effects are relatively small although one observes specific behaviors for small matrices. Indeed below 164 Ar atoms we are mostly facing an Ar cluster with an inclusion of a Na cluster, with properties strongly depending on the system size. For larger numbers of Ar atoms, we clearly see more regular patterns, hinting to a convergence of the system's properties towards a "bulk-like" limit.

In the last part of the paper, we have presented results specifically for the case of non-linear processes, especially in relation to intense laser irradiation. The surrounding Ar stops a Coulomb explosion which would else-wise have taken place due to the strong laser ionization of the cluster. Steady shape oscillations of the cluster are then observed, while the absorbed momentum spreads in a radial sound wave propagating through the atoms and triggers global radial oscillations thereof. The relaxation process can be nicely seen in oscillations of cluster radius and deformation. Both these observables lead to unique signatures in the plasmon spectrum of the cluster which, in turn, provides an ideal handle for pump and probe analysis. More investigations are in progress to quantify these effects.

In this paper, we have focused mainly on the actual response of the Na cluster itself, not discussing deeply the induced impact on the matrix. It should thus be highly interesting to investigate the impact of this emission and/or energy deposit on the matrix itself. Our model was originally tailored for this purpose and it is

indeed well suited to it. We shall present these results in a forthcoming publication. Moreover we have started some research program in the case of more realistic environments such as MgO or SiO₂. Another line of development, which we also investigate, concerns clusters and molecules of biological interest, which again have to be treated in relation to an environment, often water. Work along that line is also in progress with aim to consider the effects of irradiation on such systems.

References

1. U. Kreibig and M. Vollmer, *Optical Properties of Metal Clusters* (Springer Series in Materials Science, 1993).
2. H. Haberland (ed.), *Clusters of Atoms and Molecules 1- Theory, Experiment, and Clusters of Atoms* (Springer Series in Chemical Physics, Berlin, 1994).
3. H. Haberland (ed.), *Clusters of Atoms and Molecules 2- Solvation and Chemistry of Free Clusters, and Embedded, Supported and Compressed Clusters* (Springer Series in Chemical Physics, Berlin, 1994).
4. W. Ekardt (ed.), *Metal Clusters* (Wiley, New York, 1999).
5. P.-G. Reinhard and E. Suraud, *Introduction to Cluster Dynamics* (Wiley, New York, 2003).
6. N. Nilius, N. Ernst and H.-J. Freund, *Phys. Rev. Lett.* **84**, p. 3994 (2000).
7. M. Gaudry, J. Lermé, E. Cottancin, M. Pellarin, J.-L. Vialle, M. Broyer, B. Prével, M. Treilleux and P. Mélinon, *Phys. Rev. B* **64**, p. 085407 (2001).
8. T. Diederich, J. Tiggesbümker and K. H. Meiwes-Broer, *J. Chem. Phys.* **116**, p. 3263 (2002).
9. P. J. Mitchell and D. Fincham, *J. Phys.: Condensed Matter* **5**, p. 1031 (1993).
10. A. Nasluzov, K. Neyman, U. Birkenheuer and N. Rösch, *J. Chem. Phys.* **115**, p. 17 (2001).
11. M. J. Field, P. A. Bash and M. Karplus, *J. Comp. Chem.* **11**, p. 700 (1990).
12. J. Gao, *Acc. Chem. Res.* **29**, p. 298 (1996).
13. N. Gresh and D. R. Garmer, *J. Comp. Chem.* **17**, p. 1481 (1996).
14. F. Fehrer, P.-G. Reinhard, E. Suraud, E. Giglio, B. Gervais and A. Ipatov, *Appl. Phys. A* **82**, p. 152 (2005).
15. F. Calvayrac, P.-G. Reinhard, E. Suraud and C. A. Ullrich, *Phys. Rep.* **337**, p. 493 (2000).
16. S. Kümmel, M. Brack and P.-G. Reinhard, *Euro. Phys. J. D* **9**, p. 149 (1999).
17. B. G. Dick and A. W. Overhauser, *Phys. Rev.* **112**, p. 90 (1958).
18. G. R. Ahmadi, J. Almlöf and J. Roegen, *Chem. Phys.* **199**, p. 33 (1995).
19. F. Dupl e and F. Spiegelmann, *J. Chem. Phys.* **105**, p. 1492 (1996).
20. B. Gervais, E. Giglio, E. Jaquet, A. Ipatov, P.-G. Reinhard and E. Suraud, *J. Chem. Phys.* **121**, p. 8466 (2004).
21. F. Calvayrac, P.-G. Reinhard and E. Suraud, *Phys. Rev. B* **52**, p. R17056 (1995).
22. F. Calvayrac, P.-G. Reinhard and E. Suraud, *Ann. Phys. (NY)* **255**, p. 125 (1997).
23. K. Yabana and G. F. Bertsch, *Phys. Rev. B* **54**, p. 4484 (1996).
24. B. Montag and P.-G. Reinhard, *Phys. Lett. A* **193**, p. 380 (1994).
25. B. Montag and P.-G. Reinhard, *Z. f. Physik D* **33**, p. 265 (1995).
26. P.-G. Reinhard and E. Suraud, *Euro. Phys. J. D* **21**, p. 315 (2002).
27. F. Fehrer, P.-G. Reinhard and E. Suraud, *Appl. Phys. A* **82**, p. 145 (2005).
28. V. Vorsa, P. Campagnola, S. Nandi, M. Larsson and W. Lineberger, *J. Chem. Phys.* **105**, p. 2298 (1996).
29. K. Andrae, P.-G. Reinhard and E. Suraud, *J. Phys. B* **35**, p. 1 (2002).

30. K. Andrae, P.-G. Reinhard and E. Suraud, *Phys. Rev. Lett.* **92**, p. 173402 (2004).
31. G. Seifert, M. Kaempfe, K.-J. Berg and H. Graener, *Appl. Phys. B* **71**, p. 795 (2000).